Br J Dermatol 2025; **192**:335–343
https://doi.org/10.1093/bjd/ljae386
Advance access publication date: 11 October 2024

BJD
British Journal of Dermatology
General Dermatology

Comprehensive mutational profiling identifies new driver events in cutaneous leiomyosarcoma

Louise van der Weyden,[1] Martin Del Castillo Velasco-Herrera,[1] Saamin Cheema,[1] Kim Wong,[1] Jacqueline M Boccacino,[1] Victoria Offord,[1] Alastair Droop,[1] David RA Jones,[1] Ian Vermes,[1] Elizabeth Anderson,[1] Claire Hardy,[1] Nicolas de Saint Aubain,[2] Peter M Ferguson,[3,4,5] Emily L Clarke,[6,7] William Merchant,[6] Carolin Mogler,[8] Derek Frew,[9] Paul W Harms,[10] Carlos Monteagudo,[11,12] Steven D Billings,[9] Mark J Arends,[13] Ingrid Ferreira,[1] Thomas Brenn[10] and David J Adams[1]

[1]Wellcome Sanger Institute, Wellcome Genome Campus, Hinxton, UK
[2]Department of Pathology, Institut Jules Bordet, Université Libre de Bruxelles, Brussels, Belgium
[3]Tissue Pathology and Diagnostic Oncology, Royal Prince Alfred Hospital and NSW Health Pathology, Sydney, NSW, Australia
[4]Faculty of Medicine and Health, The University of Sydney, Sydney, NSW, Australia
[5]Melanoma Institute Australia, The University of Sydney, Sydney, NSW, Australia
[6]Department of Histopathology, Leeds Teaching Hospitals NHS Trust, Leeds, UK
[7]Division of Pathology and Data Analytics, University of Leeds, Leeds, UK
[8]Institute of Pathology, School of Medicine and Health, Technical University Munich, Munich, Germany
[9]Department of Pathology, Robert J. Tomsich Pathology and Laboratory Medicine Institute, Cleveland Clinic, Cleveland, OH, USA
[10]Departments of Pathology and Dermatology, University of Michigan, Ann Arbor, MI, USA
[11]Department of Pathology, University Clinic Hospital, Valencia – INCLIVA Biomedical Research Institute, Valencia, Spain
[12]Department of Pathology, University of Valencia, Valencia, Spain
[13]University of Edinburgh, Division of Pathology, Centre for Comparative Pathology, CRUK Edinburgh Centre, Institute of Genetics and Cancer, Western General Hospital, Edinburgh, UK

Correspondence: David J. Adams. Email: da1@sanger.ac.uk

Abstract

Background Cutaneous leiomyosarcoma (cLMS) is a rare soft-tissue neoplasm, showing smooth muscle differentiation, that arises from the mesenchymal cells of the dermis. To date, genetic investigation of these tumours has involved studies with small sample sizes and limited analyses that identified recurrent somatic mutations in *RB1* and *TP53*, copy number gain of *MYOCD* and *IGF1R*, and copy number loss of *PTEN*.

Objectives To better understand the molecular pathogenesis of cLMS, we comprehensively explored the mutational landscape of these rare tumours to identify candidate driver events.

Methods In this retrospective, multi-institutional study, we performed whole-exome sequencing and RNA sequencing in 38 cases of cLMS.

Results *TP53* and *RB1* were identified as significantly mutated and thus represent validated driver genes of cLMS. COSMIC mutational signatures SBS7a/b and DBS1 were recurrent; thus, ultraviolet light exposure may be an aetiological factor driving cLMS. Analysis of significantly recurrent somatic copy number alterations, which represent candidate driver events, found focal (< 10 Mb) deletions encompassing *TP53* and *KDM6B*, and amplifications encompassing *ZMYM2*, *MYOCD*, *MAP2K4* and *NCOR1*. A larger (24 Mb) recurrent deletion encompassing *CYLD* was also identified as significant. Significantly recurrent broad copy number alterations, involving at least half of a chromosome arm, included deletions of 6p/q, 10p/q, 11q, 12q, 13q and 16p/q, and amplification of 15q. Notably *PTEN* is located on 10q, *RB1* on 13q and *IGFR1* on 15q. Fusion gene analysis identified recurrent *CRTC1/CRTC3::MAML2* fusions, as well as many novel fusions in individual samples.

Conclusions Our analysis of the largest number of cases of cLMS to date highlights the importance of large cohort sizes and exploration beyond small targeted gene panels when performing molecular analyses, as it allowed a comprehensive exploration of the mutational landscape of these tumours and identification of novel candidate driver events. It also uniquely afforded the opportunity to compare the molecular phenotype of cLMS with LMS of other tissue types, such as uterine and soft-tissue LMS. Given that molecular profiling has resulted in the development of novel targeted treatment approaches for uterine and soft-tissue LMS, our study now allows the same opportunities to become available for patients with cLMS.

Accepted: 30 September 2024
© The Author(s) 2024. Published by Oxford University Press on behalf of British Association of Dermatologists. All rights reserved. For commercial re-use, please contact reprints@oup.com for reprints and translation rights for reprints. All other permissions can be obtained through our RightsLink service via the Permissions link on the article page on our site—for further information please contact journals.permissions@oup.com.

Lay summary

Cutaneous leiomyosarcoma (or 'cLMS' for short) is a type of skin tumour. It commonly appears as a painful nodule on the trunk, legs or arms. Surgery to remove it is recommended, but it can grow back and may spread to other organs. For this reason, we need to understand more about cLMS to try to find other treatments.

Analysing the genetic material in tumour cells lets us know which genes have been mutated or altered. This is important as these mutations or alterations can play a role in the development of a tumour or its progression. Recording all the mutations and alterations found in a tumour is crucial to understanding the biology of the disease. It is also important in finding ways to diagnose the disease, predicting how it will progress and finding treatments for it.

Up to now, only two studies have analysed the genetic material in cLMS tumours. Samples were only available from small groups of people and fewer than 100 genes were investigated. To study the genetic changes in cLMS and identify the key events that cause them, we analysed all the genes in the DNA of a large number of people with cLMS. We confirmed that two genes (called '*TP53*' and '*RB1*') could be key to the development of cLMS. We also found new possible causes of cLMS, including exposure to sunlight, changes in chromosomes and some gene fusions.

These findings give us a better understanding of the biology of cLMS.

What is already known about this topic?

- Only two studies have performed next-generation sequencing of cutaneous leiomyosarcoma (cLMS), with both limited by targeted panel sequencing (< 100 cancer genes) and small cohorts (n=5–11 samples).
- Recurrent somatic mutations were found in *TP53* and *RB1*.
- Copy number loss of *PTEN* and *MYOCD*, and copy number gain of *IGFR1* have also been reported.
- No mutational signature analyses were performed and no fusion genes were found.

What does this study add?

- Whole-exome sequencing a large cohort allowed validation of *TP53* and *RB1* as cLMS driver genes.
- We identified novel putative driver events: ultraviolet exposure, significantly recurrent focal copy number alterations (deletions encompassing *TP53* and *KDM6B*, and amplifications encompassing *ZMYM2*, *MYOCD*, *MAP2K4* and *NCOR1*), significantly recurrent chromosomal arm gains/losses (encompassing *PTEN* and *RB1*) and recurrent fusion genes (*CRTC1/CRTC3::MAML2*).
- We compared the mutational landscape with leiomyosarcoma of other tissues.

Leiomyosarcoma (LMS) is a malignant soft-tissue neoplasm that shows smooth muscle differentiation. Although most commonly of uterine or soft-tissue origin, LMS can also be found in the skin ('superficial LMS'). Superficial LMS are rare skin cancers, comprising only 2–3% of cutaneous sarcomas.[1] They can be divided into two histopathological subtypes: cutaneous/dermal LMS (cLMS; also known as 'atypical intradermal smooth muscle neoplasm'), originating from the dermally located hair follicle muscles, areolar or dartos muscles; and subcutaneous LMS, originating from the vascular muscles in the subcutaneous adipose tissue.[1,2] cLMS is the more common subtype.

cLMS most typically appears on the trunk and extremities, often presenting as a painful, solitary nodule. Although most studies associate a low risk of aggressive behaviour with cLMS, there have been reports of recurrence in up to 19–40% patients, with margin status being the most important predictor of recurrence.[3,4] Furthermore, although cLMS originates from the dermis, it can also show focal infiltration/invasion of the superficial layers of the subcutis. Importantly, invasion of the tumour into the subcutaneous tissue is considered prognostic, as even minimal subcutis involvement can be associated with late local recurrences and/or distant metastases.[5,6]

There is currently a wealth of information about the molecular features of LMS; however, they are all related to those of uterine or soft-tissue origin.[7] Indeed, to date, only two studies have performed next-generation sequencing of cLMS, and both have used targeted panels (< 100 oncogenes and tumour suppressor genes) and small cohorts (n=5–11 samples), finding only recurrent somatic mutations in *RB1* and *TP53*.[8,9] Copy number gain of *MYOCD* (in 2 of 11 samples) and *IGF1R* (in 1 of 5 samples), and loss of *PTEN* (in 1 of 5 samples) have also been reported.[8,9] Thus, the mutational landscape of cLMS remains largely unknown. To explore comprehensively the mutational landscape of these tumours and identify candidate driver events, we performed a retrospective multi-institutional whole-exome sequencing (WES) and RNA sequencing (RNA-Seq) study on the largest cohort of patients with cLMS to date (n=38).

Materials and methods

Sample collection and nucleic acid isolation

The cLMS samples consisted of formalin-fixed paraffin-embedded (FFPE) tissues collected as part of routine

diagnostic procedures. Representative haematoxylin and eosin-stained sections of all FFPE tissue blocks were independently reviewed by two specialist dermatopathologists (T.B. and I.F.) to confirm diagnoses and identify areas for sampling. The tumours were all dermal-based, with a proportion also showing invasion into the subcutis. Genomic DNA was extracted from the normal samples, and genomic DNA and RNA were extracted from the tumour samples. Extractions were done using an AllPrep DNA/RNA FFPE Kit (Qiagen, Hilden, Germany).

Sequencing, read alignment and quality control

Sequencing libraries were prepared from the FFPE-extracted DNA using a NEBNext® Ultra™ II DNA Library Prep Kit (New England Biolabs, Hitchin, UK), followed by whole-exome capture using SureSelect Human All Exon V5 baits (Agilent, Santa Clara, CA, USA). The FFPE-extracted RNA samples were reverse-transcribed and cDNA sequencing libraries prepared using the Custom mRNA Isolation and First/Second Strand Synthesis Kit (Illumina, San Diego, CA, USA), followed by whole-exome capture using SureSelect Human All Exon V5 baits (Agilent). Multiplexed libraries were paired-end sequenced using the NovaSeq6000 platform (Illumina) to generate 101-base pair reads. The DNA sequencing reads were aligned to the GRCh38 reference genome, using BWA-MEM (version 0.7.17),[10] and polymerase chain reaction (PCR) duplicates were marked using the samtools (version 1.14)[11] 'markdup' function with parameters '--mode s -S --include-fails'. Tumour–normal sample concordance, as well as tumour–normal contamination, was assessed using Conpair (version 0.2).[12] Samples were excluded on the basis of quality issues, such as having < 80% of the targeted regions covered with at least × 20 coverage or cross-individual contamination > 5% in either the tumour or matched normal. The RNA sequencing reads were aligned to the GRCh38 reference genome using STAR (version 2.5.0c15) and Ensembl (version 103) annotation.[13] Data quality was assessed by running RNA-SeqQC 2.[14] We discarded any samples that reported the following: expression profiling efficiency < 40%; 3′ bias < 0.3 or 3′ bias > 0.5; proportion of reads intersecting rRNAs > 2.5; read pairs counted as < 20 million reads; a higher total number of low-quality, ambiguous and multimapping reads than the total reads counted; or number of genes with five counts or more of < 14 000.[15]

Identification and annotation of somatic variants

Somatic mutations were identified using cgpCaVEMan (version 1.15.2) for single nucleotide variants, SmartPhase (version 1.2.1) for multinucleotide variants and cgpPindel (version 3.10.0) for insertions/deletions (indels).[16–18] A schematic overview of the filtering strategy used to identify the somatic mutations is provided in Figure S1 (see Supporting Information). Details of the methods for each algorithm, and the specific parameters, input files and flagging rules used, are provided in Appendix S1 (see Supporting Information). The Ensembl (version 103) Variant Effect Predictor (VEP) was used to predict the consequences of base changes and indels on proteins.[19] As a gene may have multiple transcripts, the canonical transcript – as defined in Ensembl – was used to determine the variant consequence. VEP was also used to add custom annotations from the COSMIC (version 97), gnomAD (version 3.1.2) and dbSNP (version 155) databases.[20–22] Memorial Sloan Kettering Cancer Center's Precision Oncology Knowledge Base, OncoKB™, was used to define 'cancer genes' (https://www.oncokb.org/cancer-genes).

Identification of somatic copy number alterations

Somatic copy number alterations (SCNAs) were identified using ASCAT (version 3.1.2).[23] This was also used to estimate the purity, ploidy and allele-specific copy number at each locus. Cases with a solution with a goodness-of-fit score < 0.9 were excluded from further analysis. The outputs from ASCAT were used to generate input files for GISTIC2 (version 2.0.23),[24] which identifies significantly recurrent SCNAs. The threshold for the residual *q*-value for both broad and focal amplifications and deletions was set at 0.10. GISTIC2 wide peaks with an overlap of > 40% with regions known to be problematic for sequencing and/or read mapping (as defined by the Genome in a Bottle Consortium benchmark union set of all difficult regions; version 3.3) were considered artefactual SCNAs and removed from the analysis. Wide peaks were also excluded if the list of samples predicted to have a particular SCNA in GISTIC2 did not concur with the original ASCAT results.

Mutational signature analysis

COSMIC mutational signature identification was performed using SigProfilerExtractor (version 1.1.21),[25] run in exome mode, using GRCh38 as the reference and opportunity genome. Results from signature decomposition and assignment were taken forward if the cosine similarity between the *de novo* extracted signatures and signatures reconstructed from assigned COSMIC signatures was ≥ 0.9. Similarly, on a per-sample basis, signature analysis was considered reliable if the cosine similarity between the original mutational spectrum and reconstructed spectrum was ≥ 0.9 and there were ≥ 100 mutations per sample, for each substitution type (single base substitutions, doublet substitutions and indels).

Identification of significantly mutated genes

To identify driver genes, we used dNdScv (version 0.0.1.0; git commit ID: 0633182),[26] which detects genes under positive selection in cancer. The reference gene annotations and covariates files used to run the algorithm were provided in the 'dNdScv' package ('RefCDS_human_GRCh38_GencodeV18_recommended.rda' and 'covariates_hg19_hg38_epigenome_pcawg.rda', respectively). The analysis was run using the 'with covariates' option. The outputs included *P*-values that were adjusted using the Benjamini–Hochberg method. The 'dNdScv' algorithm provides *q*-values for genes based on specific mutation types only (e.g. missense mutations) or all mutation types (global *q*-value). To identify significant genes, we considered those that had a global *q*-value < 0.1.

Mutual exclusivity and co-occurrence of mutated genes

The statistical test available on the OncoPrint feature of cBioPortal (http://www.cbioportal.org/oncoprinter) was used to perform co-occurrence and mutual exclusivity analysis.[27] Briefly, for gene pairs, an odds ratio (OR) is calculated and a one-sided Fisher's exact test is used to calculate significance. *P*-values are adjusted using the Benjamini–Hochberg false discovery rate correction method. A log2 OR > 0 is associated with tendency toward co-mutation, and a log2 OR ≤ 0 is associated with a tendency toward mutual exclusivity. For analysis of *TP53* and *RB1*, somatic mutations and copy number status were used. The finding of co-mutation of these genes (log2 OR > 3) was significant ($q=0.002$ when considering both mutations and copy number loss; $q=0.001$ when considering only mutations). Mutation of *TP53* or *RB1* was not mutually exclusive with significantly recurrent broad or focal SCNAs. A *q*-value threshold of 0.05 was used for significance.

Identification of fusion genes

Fusion gene identification was performed using STAR-Fusion version 1.10.1, which used STAR (version 2.78a)[28] alongside the Trinity Cancer Transcriptome Analysis Toolkit genome reference library StarFv1.10 for GRCh38 GENCODEv37 (Ensembl version 103) gene annotations. Only samples that passed the RNA-Seq quality criteria were used for gene fusion analysis. To assess the coding effect of the fusions, annotate their presence in previous databases and validate them *in silico*, we used FusionInspector version 2.6.0 by running STAR-Fusion with the parameters '--FusionInspector validate--examine_coding_effect --denovo_reconstructFusion'. Subsequently, we filtered out gene fusion predictions that had a total number of junction read counts plus spanning fragment counts < 5, fusion fragments per million < 0.1, an unknown coding effect, annotated as previously reported in normal tissues of the Genotype-Tissue Expression (GTEx) project or fusions comprised of gene neighbours.

Results

Demographics and phenotype of the cohort with cutaneous leiomyosarcoma

The cLMS cohort consisted of 38 FFPE primary tumour samples from 38 adults [26 men, 12 women; mean (SD) age 62 (14) years] from 7 institutions across 6 countries. The most common body sites were the legs, including knees ($n=13/38$; 34%), and arms ($n=6/38$; 16%) and shoulders ($n=6/38$; 16%). Histopathologically, the tumours were hypercellular, often with nodular outlines, and composed of intersecting fascicles of spindle cells with brightly eosinophilic cytoplasm containing irregular and variably hyperchromatic and vesicular nuclei with prominent nucleoli (Figure S2; see Supporting Information). Mitotic count ranged from 0 to 25 per 10 high-powered fields (HPF; median 2 per 10 HPF). The tumours were all dermally based, with 11 of 38 samples (29%) being located entirely within the dermis, 16 of 38 (42%) showing invasion into the subcutis and 11 of 38 (29%) with unknown subcutis invasion (as the sample was transected). No lymphovascular or perineural invasion was seen. Three tumours were characterized by a well-circumscribed nodular growth pattern. Eleven tumours showed a background morphologically reminiscent of pilar leiomyoma. Of the tumours for which immunohistochemistry was performed at the time of diagnosis, all showed positive staining for desmin ($n=34$), smooth muscle actin ($n=30$) and caldesmon ($n=13$). Clinical follow-up was available for 29 patients: there was one local recurrence after 12 months, but no metastases or death from disease was identified, and 25 patients are alive with no evidence of disease, with 3 dying from unrelated causes.

Whole-exome sequencing (WES) was performed on the DNA from 23 samples to profile somatic mutations, SCNA and mutational signatures, and RNAseq was performed on the RNA from 35 samples to identify fusion genes. A summary of sample details, including histopathological and clinical information, as well as which samples were used for each of the analyses, is provided in Table S1 (see Supporting Information).

TP53 and *RB1* are significantly mutated in cutaneous leiomyosarcoma

The complete list of somatic variants for the cLMS samples is provided in Table S2 (see Supporting Information). The most recurrently mutated genes were the tumour suppressor genes (TSGs), *TP53* ($n=16/23$ tumours; 69%) and *RB1* [$n=13/23$; 57% (Figure 1)], consistent with reports of targeted sequencing of a small number of cLMS.[8,9] We found that both genes were statistically significantly mutated ($q=0$ for both genes; see 'Materials and methods'), thus validating them as driver genes for cLMS. The *TP53* variants were predominantly missense or nonsense mutations, with four tumours having multiple mutations ($n=2$–3), and the *RB1* variants were predominantly nonsense mutations. Six tumours with focal copy number deletions (< 10 Mb) spanning the *TP53* locus, and two tumours with copy neutral loss of heterozygosity spanning the *TP53* locus, also had point mutations in *TP53*, thus resulting in biallelic inactivation (Figure 1). Similarly, 10 tumours with whole chromosome arm deletions of 10q, which is where *RB1* is located, also had point mutations in *RB1*, resulting in biallelic inactivation. This is notable as patients with biallelic inactivation of *TP53* or *RB1* have been linked to poorer outcomes in some tumour types.[29,30] Importantly, *TP53* and *RB1* were found to be significantly co-mutated ($q=0.002$ when considering both mutations and copy number loss; $q=0.001$ when considering only mutations), and *TP53/RB1* co-occurrence has been reported as a frequent event in nonprimary (recurrent and metastatic) LMS of soft-tissue and uterine origin (90% and 74% of cases, respectively).[31] We did not find any mutually exclusive gene pairs of statistical significance.

Significantly recurrent copy number alterations in cutaneous leiomyosarcoma

Our large cohort size allowed the identification of significantly recurrent amplification/deletion events, which

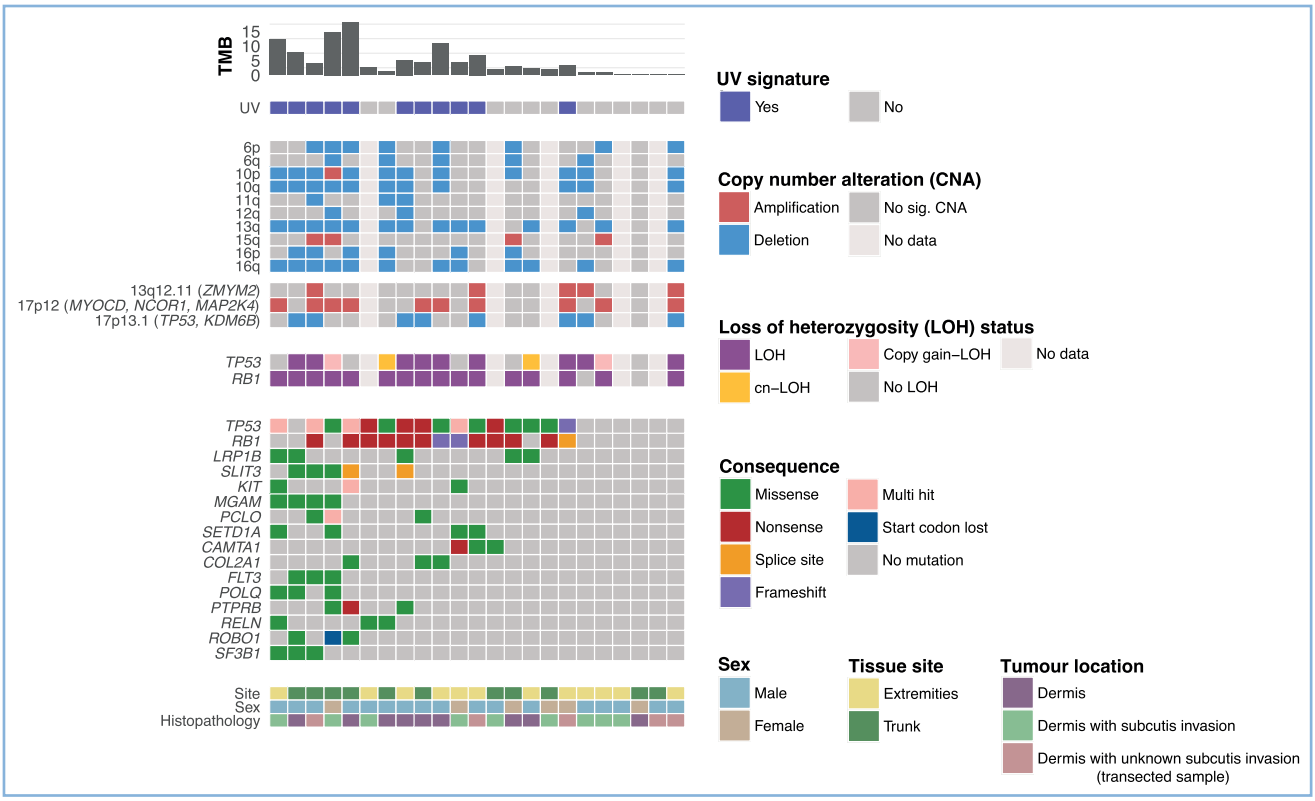

Figure 1 Overall somatic mutational landscape of cutaneous leiomyosarcoma. Tumour mutational burden (TMB) is shown as mutations per megabase. Ultraviolet (UV) signature indicates samples with the COSMIC signature SBS7. Significantly recurrent broad deletions or amplifications include the short (p) or long (q) arm of the chromosomes listed. The significantly recurrent focal copy number alterations shown include amplifications/deletions < 10 Mb in size. Specifically, the focal deletion is a 242-kb region overlapping 17p13.1 and the focal amplifications are a 0.9-Mb region within 13q12.11 and a 4.1-Mb region overlapping 17p12. Loss of heterozygosity (LOH) status is shown for *TP53* and *RB1* and includes copy number loss (LOH), copy neutral LOH (cn-LOH) and copy gain LOH. Both focal and broad copy number losses encompassing either *TP53* or *RB1* were used to determine LOH status. The oncoplot panel shows OncoKB™ cancer genes for which a mutation was present in at least three samples. *TP53* and *RB1* are significantly mutated genes. For tumour site, the locations are either the extremities (arms, hands, legs and feet) or trunk (shoulders, torso and buttocks/genital areas).

represent candidate driver events (Figure 1). Considering focal copy number alterations (< 10 Mb in size), these included a 242-kb deletion within 17p13.1 [$n=8/18$ (44%) samples; $q=6.0\times10^{-4}$] encompassing the TSGs, *TP53* and *KDM6B*, and a 0.9-Mb amplification within 13q12.11 [$n=5/18$ (28%) samples; $q=7.6\times10^{-6}$] encompassing *ZMYM2*, a gene that has been reported to be a partner in several oncogenic fusions. In addition, *MYOCD* was amplified, as reported previously,[9] overlapping a 4.1-Mb region of 17p12 [$n=10/18$ (56%) samples; $q=4.3\times10^{-8}$] that also encompassed the oncogenes *MAP2K4* and *NCOR1*. Considering copy number alterations up to half a chromosome arm in size identified a 24.3-Mb deletion on 16q [$n=14/18$ (78%) samples; $q=0.036$], within which the TSG *CYLD* is located. Considering broad copy number alterations (from half to a full chromosome arm in size), these included deletions of 6p/q, 10p/q, 11q, 12q, 13q and 16p/q, and amplification of 15q [Figure 1; Table S3 (see Supporting Information)]. Although numerous genes are located within these chromosome arms, it is worth noting that *PTEN* is located at 10q23 and *IGFR1* is located at 15q25, as copy number loss and gain of these genes, respectively, have been previously reported in cLMS (in 1 of 5 samples each).[8]

Ultraviolet exposure may drive a subset of cutaneous leiomyosarcoma

The median tumour mutational burden of cLMS was 2.28 mutations per Mb (range 0.06–14.04; Figure 1). We were able to identify COSMIC mutational signatures SBS7a and/or SBS7b, which are comprised primarily of C > T mutations, in 11 of 23 samples [Figure 1; Table S4 (see Supporting Information)]. In four of these cases, signature DBS1, comprised of CC > TT, was also identified (Table S4). SBS7/DBS1 are attributed to ultraviolet (UV) light, thus UV exposure may be an aetiological factor in driving a subset of cLMS.

Identification of fusion genes found in cutaneous leiomyosarcoma

Fusion genes are an important class of driver event in cancer that can play a role in both cancer initiation and progression. A total of 32 different fusion genes were identified in our cLMS cohort, and included both frameshift fusions ($n=8$) and in-frame fusions [$n=24$; Table S5 (see Supporting Information)]. The recurrent fusion genes were *CRTC1::MAML2* ($n=3$) and *CRTC3::MAML2* ($n=2$), which have also been reported in other tumour types,[32–36] but we

are the first to report these fusions in cLMS. The breakpoints for these fusions were different between the individual tumours; however, the resulting transcript involved exons 1–3 of *CRTC1* or exons 1–2 of *CRTC3* being spliced to exons 2–5 of *MAML2* (Figure 2). In addition, two of the tumours also contained the reciprocal fusion (i.e., *MAML2::CRTC1* or *MAML2::CRTC3*), which have not previously been reported. The rest of the fusions ($n=28$) were not recurrent. These included *YAP1::MAML2* and *YAP1::NUTM1*, which are recurrent in poromas and porocarcinomas.[37] Others included those that have been identified by large-scale analyses of The Cancer Genome Atlas datasets and found to be present in a single sample, such as *PER3::CAMTA1* in head-and-neck squamous cell carcinoma and *BCL2L13::SPECC1* in hepatocellular carcinoma.[38,39] The remainder have not previously been reported.

Discussion

This study is the first to unveil the mutational landscape of cLMS, which allows for a comparison with LMS of other tissue types. Similarities between cLMS, uterine LMS (uLMS) and soft-tissue LMS (stLMS) include the identification of *TP53* and *RB1* as significantly mutated genes (SMGs).[8,40–43] Importantly, we also found frequent biallelic inactivation of *TP53* and *RB1* and the co-occurrence of *TP53* and *RB1* mutations in our samples, which has been reported in uLMS and stLMS.[31,41] *ATRX* has been identified as an SMG in a cohort of primary and metastatic LMS from a variety of tissue sites,[41] with *ATRX* and *PTEN* identified as SMGs in uLMS.[42,43] In our cLMS cohort, an *ATRX* mutation was only found in 1 of 23 samples; however, while we did not find any point mutations in *PTEN*, which is located at 10q23, a significantly recurrent loss of chromosome 10q was seen. Recurrent *MED12* mutations have also been reported in uLMS (up to 30% frequency);[42,44–49] however, we did not see any *MED12* mutations in our cLMS cohort.

uLMS and LMS from a variety of tissue sites are characterized by widespread SCNA with multiple cancer drivers affected,[41–43] which is similar to the SCNA landscape of cLMS. Specifically, the significant focal deletions on 17p encompassing TSG *TP53* (resulting in biallelic inactivation of *TP53* in several cases), and significant focal amplifications on 17p encompassing the oncogenes *MAP2K4* and *NCOR1*, have also reported in uLMS and LMS from a variety of tissue sites.[41–43,49] The amplification of *MAP2K4* in cLMS is of interest as a novel MAP2K4 inhibitor has recently shown promising *in vivo* activity against patient-derived xenograft models of uLMS with copy number amplification of *MAP2K4* (found in up to 30% of cases),[50] suggesting that patients with cLMS with *MAP2K4* amplifications may also benefit from this treatment.

The focal amplification on 17p12 seen in 30% of uLMS cases has been reported to encompass *MYOCD*,[42] as did the 17p12 focal amplification seen in our cLMS samples. Interestingly, amplification of *MYOCD* has also been reported in retroperitoneal LMS.[51] Although *MYOCD* is not classified as an oncogene, upregulation of *MYOCD* increases epithelial–mesenchymal transition and promotes cell invasion in gastric cancer,[52,53] and high expression of *MYOCD* is associated with decreased survival in people with lung cancer.[54] Interestingly, molecular investigation of a uterine leiomyoma that metastasized to the lung reported an amplification at 17p12 encompassing *MAP2K3* and *MYOCD* in the lung metastases that were classified as LMS, but not the primary leiomyoma,[55] further implicating a role for *MYOCD* in tumour progression.

When considering significant SCNAs within broader copy number alterations, the TSG *CYLD* was identified within a 24.3-Mb deletion on chromosome 16q in 12 of 18 samples, and frequent copy number deletions spanning *CYLD* have been reported in uLMS (35% of cases).[42] Loss of 13q was significantly recurrent in our cLMS cohort, and has also been recurrently observed in uLMS and cohorts of LMS from a variety of body sites.[56–58] Similarly, loss of 10q was significantly recurrent in our cohort, and has also been recurrently observed in uLMS, stLMS and cohorts of LMS from a variety of body sites.[49,56–60] It is worth noting that loss of 10q in both uterine and extrauterine LMS is associated with aggressive

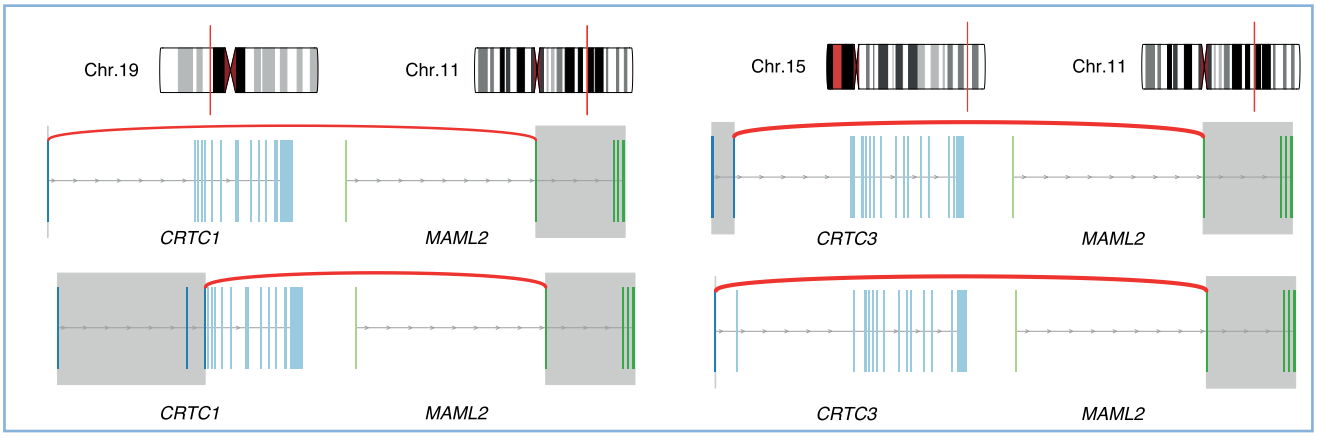

Figure 2 *CRTC1::MAML2* and *CRTC3::MAML2* fusion genes in cutaneous leiomyosarcoma. Schematic of the *CRTC1::MAML2* and *CRTC3::MAML2* fusions found in two representative cutaneous leiomyosarcoma samples. The vertical red bars on the chromosome images denote the location of the gene within the chromosome. The grey blocks on the gene images represent the exons that are present in the gene fusion that is formed, with the red arc representing the joining of the two genes. The breakpoints for these interchromosomal fusions were different between the individual tumours; however, the resulting transcript involved exons 1–3 of *CRTC1* or 1–2 of *CRTC3* being spliced to exons 2–5 of *MAML2*. Chr., chromosome.

behaviour, typically being found in high-grade and/or recurrent tumours.[56,58] Interestingly, the only sample in our cohort from a patient that developed a recurrence (12 months post-diagnosis) did not show any loss of 10q. However, that sample showed biallelic loss of both *TP53* and *RB1*.

Fusion genes are an important class of driver event in cancer that can play a role in both cancer initiation and progression; thus, they can represent a key part of the mutational landscape of a tumour. The recurrent *CRTC1/CRTC3::MAML2* fusion genes we identified in five cLMS tumours, two of which also carried the reciprocal fusion (*MAML2::CRTC1/CRTC3*), are of interest. Although there have been no previous reports of the reciprocal fusions, the *CRTC1/CRTC3::MAML2* fusion genes have been reported in hidradenoma at a frequency of 26–50% and 5% frequency, respectively,[32,36] as well as in mucoepidermoid carcinoma (MEC) of the salivary gland and tracheobronchial tree (30–80% and approximately 6% frequency of each fusion gene, respectively).[33–35] Studies using reverse transcription PCR have shown that the fusion involves exons 1 of *CRTC1* or *CRTC3* being fused inframe to exons 2–5 of *MAML2*,[36,61] similar to that seen our cLMS cohort. The *CRTC1::MAML2* fusion gene, formed by fusion of the cAMP response element-binding (CREB)-binding domain of CREB coactivator *CRTC1* and the transactivation domain of Notch coactivator *MAML2*, has been shown to exhibit transforming activity *in vitro* and *in vivo* and is reported to be the major oncogenic driver in MEC.[62] Thus, our findings suggest that similar mechanisms of tumorigenesis may exist in a portion of cLMS cases.

A limitation of our study was the use of WES rather than whole-genome sequencing. As such, we can only report on mutations within splice site and exonic regions of the genome. Although the exome is estimated to harbour approximately 85% of mutations with large effects on disease-related traits,[63] we will not have uncovered mutations in regions such as introns, promoters and other regulatory regions. In addition, future molecular profiling studies of LMS arising in the skin would benefit from including cases of subcutaneous LMS to identify genetic differences that may account for its more aggressive nature relative to cLMS.[2]

Our understanding of uLMS and stLMS pathophysiology has occurred through molecular profiling of these tumours to identify key driver events, thereby facilitating the development of novel targeted treatment approaches.[64] Similarly, the development of successful treatments for cLMS is contingent upon a thorough understanding of the molecular profile of these tumours. Our comprehensive characterization of the genomic landscape of a large cohort of cLMS has allowed, for the first time, confirmation of *TP53* and *RB1* as driver genes, and identification of copy number alterations and fusion genes that represent novel driver events. Additionally, our genetic profiling allowed for a comparison of cLMS with the well-characterized uLMS and stLMS. Thus, our findings will help in the development of novel targeted approaches for the treatment of cLMS and add to the richness of our understanding of the pathophysiology of LMS.

Acknowledgements

The Genotype-Tissue Expression (GTEx) Project was supported by the Common Fund of the Office of the Director of the National Institutes of Health, and by the National Cancer Institute; the National Human Genome Research Institute; the National Heart, Lung, and Blood Institute; the National Institute on Drug Abuse; the National Institute of Mental Health; and the National Institute of Neurological Disorders and Stroke. The authors thank Thomas Clarke (CASM information technology team, Wellcome Sanger Institute) for their help with setting up the Cancer Genome Project Insertion/Deletion detection pipeline based around Pindel.

Funding sources

This study was supported by a Medical Research Council programme grant to D.J.A. (MR/V000292/1) and the Wellcome Trust (220540/Z/20/A). For the purpose of Open Access, the author has applied a CC BY public copyright licence to any Author Accepted Manuscript version arising from this submission.

Conflicts of interest

The authors declare no conflicts of interest.

Data availability

The sequencing data are available in the European Genome and Phenome Archive repository (https://www.ebi.ac.uk/ena/browser/home) under the study accessions EGAD00001014789 for whole-exome data and EGAD00001014790 for RNA sequencing data.

Ethics statement

Ethical approval for the use of all patient samples in this project was obtained by a local committee at the institution of origin and from Research Governance at the Wellcome Sanger Institute. This study is part of the DERMATLAS Project that has been approved by the National Health Service Health Research Authority (Research Ethics Committee reference: 21/PR/1024, IRAS project ID: 304621). Patient data were anonymized.

Patient consent

Patient consent was given for the inclusion of tissue samples and associated clinical metadata in the study.

Supporting Information

Additional Supporting Information may be found in the online version of this article at the publisher's website.

References

1 Helbig D, Dippel E, Erdmann M *et al.* S1-guideline cutaneous and subcutaneous leiomyosarcoma. *J Dtsch Dermatol Ges* 2023; **21**:555–63.
2 Bresler SC, Gosnell HL, Ko JS *et al.* Subcutaneous leiomyosarcoma: an aggressive malignancy portending a significant risk of metastasis and death. *Am J Surg Pathol* 2023; **47**:1417–24.

3 Fields JP, Helwig EB. Leiomyosarcoma of the skin and subcutaneous tissue. *Cancer* 1981; **47**:156–69.
4 Kraft S, Fletcher CD. Atypical intradermal smooth muscle neoplasms: clinicopathologic analysis of 84 cases and a reappraisal of cutaneous "leiomyosarcoma". *Am J Surg Pathol* 2011; **35**:599–607.
5 Massi D, Franchi A, Alos L *et al.* Primary cutaneous leiomyosarcoma: clinicopathological analysis of 36 cases. *Histopathology* 2010; **56**:251–62.
6 Carr MJ, Sun J, Adams WA *et al.* Grade of primary cutaneous leiomyosarcoma dictates risk for metastatic spread and disease-specific mortality. *Cancer Control* 2023; **30**:10732748231206957.
7 Cope BM, Traweek RS, Lazcano R *et al.* Targeting the molecular and immunologic features of leiomyosarcoma. *Cancers (Basel)* 2023; **15**:2099.
8 Miller TI, Zoumberos NA, Johnson B *et al.* A genomic survey of sarcomas on sun-exposed skin reveals distinctive candidate drivers and potentially targetable mutations. *Hum Pathol* 2020; **102**:60–9.
9 Planet C, Dalle S, Dereure O *et al.* Clinicopathologic and molecular analyses of cutaneous leiomyosarcoma: a retrospective, multicenter study of 79 cases. *J Am Acad Dermatol* 2023; **88**:215–16.
10 Li H. Aligning sequence reads, clone sequences and assembly contigs with BWA-MEM. *arXiv.* Available at: https://arxiv.org/abs/1303.3997 (last accessed 21 October 2024).
11 Li H, Handsaker B, Wysoker A *et al.* The Sequence Alignment/Map format and SAMtools. *Bioinformatics* 2009; **25**:2078–9.
12 Bergmann EA, Chen BJ, Arora K *et al.* Conpair: concordance and contamination estimator for matched tumor-normal pairs. *Bioinformatics* 2016; **32**:3196–8.
13 Dobin A, Davis CA, Schlesinger F *et al.* STAR: ultrafast universal RNA-seq aligner. *Bioinformatics* 2013; **29**:15–21.
14 Graubert A, Aguet F, Ravi A *et al.* RNA-SeQC 2: efficient RNA-seq quality control and quantification for large cohorts. *Bioinformatics* 2021; **37**:3048–50.
15 Tarazona S, García-Alcalde F, Dopazo J *et al.* Differential expression in RNA-seq: a matter of depth. *Genome Res* 2011; **21**:2213–23.
16 Jones D, Raine KM, Davies H *et al.* cgpCaVEManWrapper: simple execution of CaVEMan in order to detect somatic single nucleotide variants in NGS data. *Curr Protoc Bioinformatics* 2016; **56**:15.10.1–.10.18.
17 Hager P, Mewes HW, Rohlfs M *et al.* SmartPhase: accurate and fast phasing of heterozygous variant pairs for genetic diagnosis of rare diseases. *PLOS Comput Biol* 2020; **16**:e1007613.
18 Raine KM, Hinton J, Butler AP *et al.* cgpPindel: identifying somatically acquired insertion and deletion events from paired end sequencing. *Curr Protoc Bioinformatics* 2015; **52**:15.7.1–.7.12.
19 McLaren W, Gil L, Hunt SE *et al.* The Ensembl variant effect predictor. *Genome Biol* 2016; **17**:122.
20 Tate JG, Bamford S, Jubb HC *et al.* COSMIC: the Catalogue Of Somatic Mutations In Cancer. *Nucleic Acids Res* 2019; **47**:D941–7.
21 Chen S, Francioli LC, Goodrich JK *et al.* A genomic mutational constraint map using variation in 76,156 human genomes. *Nature* 2024; **625**:92–100.
22 Sherry ST, Ward M, Sirotkin K. dbSNP-database for single nucleotide polymorphisms and other classes of minor genetic variation. *Genome Res* 1999; **9**:677–9.
23 Van Loo P, Nordgard SH, Lingjærde OC *et al.* Allele-specific copy number analysis of tumors. *Proc Natl Acad Sci U S A* 2010; **107**:16910–15.
24 Mermel CH, Schumacher SE, Hill B *et al.* GISTIC2.0 facilitates sensitive and confident localization of the targets of focal somatic copy-number alteration in human cancers. *Genome Biol* 2011; **12**:R41.
25 Islam SMA, Díaz-Gay M, Wu Y *et al.* Uncovering novel mutational signatures by de novo extraction with SigProfilerExtractor. *Cell Genom* 2022; **2**:100179.
26 Martincorena I, Raine KM, Gerstung M *et al.* Universal patterns of selection in cancer and somatic tissues. *Cell* 2017; **171**:1029–41.
27 Gao J, Aksoy BA, Dogrusoz U *et al.* Integrative analysis of complex cancer genomics and clinical profiles using the cBioPortal. *Sci Signal* 2013; **6**:pl1.
28 Haas BJ, Dobin A, Li B *et al.* Accuracy assessment of fusion transcript detection via read-mapping and de novo fusion transcript assembly-based methods. *Genome Biol* 2019; **20**:213.
29 Chavan SS, He J, Tytarenko R *et al.* Bi-allelic inactivation is more prevalent at relapse in multiple myeloma, identifying RB1 as an independent prognostic marker. *Blood Cancer J* 2017; **7**:e535.
30 Walker BA, Mavrommatis K, Wardell CP *et al.* A high-risk, double-hit, group of newly diagnosed myeloma identified by genomic analysis. *Leukemia* 2019; **33**:159–70.
31 Schaefer IM, Lundberg MZ, Demicco EG *et al.* Relationships between highly recurrent tumor suppressor alterations in 489 leiomyosarcomas. *Cancer* 2021; **127**:2666–73.
32 Winnes M, Mölne L, Suurküla M *et al.* Frequent fusion of the CRTC1 and MAML2 genes in clear cell variants of cutaneous hidradenomas. *Genes Chromosomes Cancer* 2007; **46**:559–63.
33 Nakayama T, Miyabe S, Okabe M *et al.* Clinicopathological significance of the CRTC3–MAML2 fusion transcript in mucoepidermoid carcinoma. *Mod Pathol* 2009; **22**:1575–81.
34 Saade RE, Bell D, Garcia J *et al.* Role of CRTC1/MAML2 translocation in the prognosis and clinical outcomes of mucoepidermoid carcinoma. *JAMA Otolaryngol Head Neck Surg* 2016; **142**:234–40.
35 Birkeland AC, Foltin SK, Michmerhuizen NL *et al.* Correlation of Crtc1/3-Maml2 fusion status, grade and survival in mucoepidermoid carcinoma. *Oral Oncol* 2017; **68**:5–8.
36 Kuma Y, Yamada Y, Yamamoto H *et al.* A novel fusion gene CRTC3–MAML2 in hidradenoma: histopathological significance. *Hum Pathol* 2017; **70**:55–61.
37 Sekine S, Kiyono T, Ryo E *et al.* Recurrent YAP1–MAML2 and YAP1–NUTM1 fusions in poroma and porocarcinoma. *J Clin Invest* 2019; **129**:3827–32.
38 Gao Q, Liang WW, Foltz SM *et al.* Driver fusions and their implications in the development and treatment of human cancers. *Cell Rep* 2018; **23**:227–38.
39 Hu X, Wang Q, Tang M *et al.* TumorFusions: an integrative resource for cancer-associated transcript fusions. *Nucleic Acids Res* 2018; **46**:D1144–9.
40 Cancer Genome Atlas Research Network. Comprehensive and integrated genomic characterization of adult soft tissue sarcomas. *Cell* 2017; **171**:950–65.
41 Chudasama P, Mughal SS, Sanders MA *et al.* Integrative genomic and transcriptomic analysis of leiomyosarcoma. *Nat Commun* 2018; **9**:144.
42 Choi J, Manzano A, Dong W *et al.* Integrated mutational landscape analysis of uterine leiomyosarcomas. *Proc Natl Acad Sci U S A* 2021; **118**:e2025182118.
43 Nacev BA, Sanchez-Vega F, Smith SA *et al.* Clinical sequencing of soft tissue and bone sarcomas delineates diverse genomic landscapes and potential therapeutic targets. *Nat Commun* 2022; **13**:3405.
44 Pérot G, Croce S, Ribeiro A *et al.* MED12 alterations in both human benign and malignant uterine soft tissue tumors. *PLOS ONE* 2012; **7**:e40015.
45 Kämpjärvi K, Mäkinen N, Kilpivaara O *et al.* Somatic MED12 mutations in uterine leiomyosarcoma and colorectal cancer. *Br J Cancer* 2012; **107**:1761–5.
46 Ravegnini G, Mariño-Enriquez A, Slater J *et al.* MED12 mutations in leiomyosarcoma and extrauterine leiomyoma. *Mod Pathol* 2013; **26**:743–9.
47 Schwetye KE, Pfeifer JD, Duncavage EJ. MED12 exon 2 mutations in uterine and extrauterine smooth muscle tumors. *Hum Pathol* 2014; **45**:65–70.

48 Mäkinen N, Mehine M, Tolvanen J *et al.* MED12, the mediator complex subunit 12 gene, is mutated at high frequency in uterine leiomyomas. *Science* 2011; **334**:252–5.
49 Cuppens T, Moisse M, Depreeuw J *et al.* Integrated genome analysis of uterine leiomyosarcoma to identify novel driver genes and targetable pathways. *Int J Cancer* 2018; **142**:1230–43.
50 McNamara B, Harold J, Manavella D *et al.* Uterine leiomyosarcomas harboring MAP2K4 gene amplification are sensitive in vivo to PLX8725, a novel MAP2K4 inhibitor. *Gynecol Oncol* 2023; **172**:65–71.
51 Pérot G, Derré J, Coindre JM *et al.* Strong smooth muscle differentiation is dependent on myocardin gene amplification in most human retroperitoneal leiomyosarcomas. *Cancer Res* 2009; **69**:2269–78.
52 Tong X, Wang S, Lei Z *et al.* MYOCD and SMAD3/SMAD4 form a positive feedback loop and drive TGF-β-induced epithelial–mesenchymal transition in non-small cell lung cancer. *Oncogene* 2020; **39**:2890–904.
53 Su F, Xiao R, Chen R *et al.* WIPF1 promotes gastric cancer progression by regulating PI3 K/Akt signaling in a myocardin-dependent manner. *iScience* 2023; **26**:108273.
54 Li P, Yuan H, Kuang X *et al.* Network module function enrichment analysis of lung squamous cell carcinoma and lung adenocarcinoma. *Medicine (Baltimore)* 2022; **101**:e31798.
55 Ahvenainen T, Khamaiseh S, Alkodsi A *et al.* Lung metastases and subsequent malignant transformation of a fumarate hydratase-deficient uterine leiomyoma. *Exp Mol Pathol* 2022; **126**:104760.
56 Hu J, Khanna V, Jones M *et al.* Genomic alterations in uterine leiomyosarcomas: potential markers for clinical diagnosis and prognosis. *Genes Chromosomes Cancer* 2001; **31**:117–24.
57 Raish M, Khurshid M, Ansari MA *et al.* Analysis of molecular cytogenetic alterations in uterine leiomyosarcoma by array-based comparative genomic hybridization. *J Cancer Res Clin Oncol* 2012; **138**:1173–86.
58 Hu J, Rao UN, Jasani S *et al.* Loss of DNA copy number of 10q is associated with aggressive behavior of leiomyosarcomas: a comparative genomic hybridization study. *Cancer Genet Cytogenet* 2005; **161**:20–7.
59 Larramendy ML, Kaur S, Svarvar C *et al.* Gene copy number profiling of soft-tissue leiomyosarcomas by array-comparative genomic hybridization. *Cancer Genet Cytogenet* 2006; **169**:94–101.
60 Derré J, Lagacé R, Nicolas A *et al.* Leiomyosarcomas and most malignant fibrous histiocytomas share very similar comparative genomic hybridization imbalances: an analysis of a series of 27 leiomyosarcomas. *Lab Invest* 2001; **81**:211–15.
61 Tonon G, Modi S, Wu L *et al.* t(11;19)(q21;p13) translocation in mucoepidermoid carcinoma creates a novel fusion product that disrupts a Notch signaling pathway. *Nat Genet* 2003; **33**:208–13.
62 Chen Z, Ni W, Li JL *et al.* The CRTC1–MAML2 fusion is the major oncogenic driver in mucoepidermoid carcinoma. *JCI Insight* 2021; **6**:e139497.
63 Majewski J, Schwartzentruber J, Lalonde E *et al.* What can exome sequencing do for you? *J Med Genet* 2011; **48**:580–9.
64 Lacuna K, Bose S, Ingham M *et al.* Therapeutic advances in leiomyosarcoma. *Front Oncol* 2023; **13**:1149106.